Inorg. Chem. **2009**, *48*, 3650−3659

Aluminoborates with Open Frameworks: Syntheses, Structures, and Properties

Cheng Rong,[†] Zhiwu Yu,[‡] Qiang Wang,[‡] Shou-Tian Zheng,[†] Chun-Yang Pan,[†] Feng Deng,*[,‡] and Guo-Yu Yang*[,†]

State Key Laboratory of Structural Chemistry, Fujian Institute of Research on the Structure of Matter, Chinese Academy of Sciences, Fuzhou, Fujian 350002, China, and State Key Laboratory of Magnetic Resonance and Atomic and Molecular Physics, Wuhan Center for Magnetic Resonance, Wuhan Institute of Physics and Mathematics, Chinese Academy of Sciences, Wuhan, Hubei 430071, China

Received November 5, 2008

Five aluminoborates $Al[B_5O_{10}]\cdot H_2dab\cdot 2H_2O$ (**1**), $[Al(B_4O_9)(BO)]\cdot H_2en$ (**2**), $[Al(B_4O_9)(BO)]\cdot H_2dap$ (**3**), $K_2Al[B_5O_{10}]\cdot 4H_2O$ (**4**), and $(NH_4)_2Al[B_5O_{10}]\cdot 4H_2O$ (**5**) have been synthesized under hydrothermal conditions and characterized by means of elemental analysis, IR, TG analysis, MAS NMR, UV−vis and fluorescence spectroscopy, powder X-ray diffraction, single-crystal X-ray diffraction, and NLO determination. The structure **1** comprises of AlO_4 tetrahedra and B_5O_{10} clusters and contains 12-, 11-, and 8-MR 3D-intersecting channels with a CrB_4 topological net. Structures **2** and **3** are both constructed from the same AlB_5O_{13} clusters and exhibit a six-connected framework with $4^{12}6^3$ topology. Structures **4** and **5** are isomorphous and are composed of AlO_4 tetrahedra and B_5O_{10} clusters that possess odd 11-MR channels and 8-MR helical channels. Structures **2**−**5** crystallized in an acentric structure and presented good SHG properties. UV−vis spectral investigation indicates that they are wide-band-gap semiconductors. The electronic structure calculations for the compounds also have been performed.

Introduction

Solid borate materials have attracted much research interest due to their rich structural chemistry and diverse applications in mineralogy and industry.[1] In terms of their chemistry, boron atoms coordinate with oxygen not only in three-fold (triangular, BO_3) but also in four-fold coordination (tetrahedral, BO_4). These BO_3 and BO_4 can further polymerize to many kinds of large oxoborate clusters through common corners (oxygen atoms).[2] Such polyanion clusters can be considered as the secondary building units (SBUs) to take part in the construction of novel borates. In the past seven decades, borates have formed the following systems: main group and transition metal (TM) borates,[2] rare earth borates,[3] and organically[4] and TM-complex[5] templated borates. Most metal borates were made by high-temperature solid-state methods or boric acid flux methods. However, organic or

* To whom correspondence should be addressed. E-mail: ygy@fjirsm.ac.cn (G.Y.Y.), dengf@wipm.ac.cn (F.D.). Fax: (+86) 591-8371-0051 (G.Y.Y.), (+86) 27-87199291, (F.D.).

† Fujian Institute of Research on the Structure of Matter, Chinese Academy of Sciences.

‡ Wuhan Institute of Physics and Mathematics, Chinese Academy of Sciences.

(1) (a) Christ, C. L.; Clark, J. R. *Phys. Chem. Miner.* **1977**, *2*, 59. (b) Burns, P. C. *Can. Mineral.* **1995**, *33*, 1167. (c) Burns, P. C.; Grice, J. D.; Hawthorne, F. C. *Can. Mineral.* **1995**, *33*, 1131. (d) Grice, J. D.; Burns, P. C.; Hawthorne, F. C. *Can. Mineral.* **1999**, *37*, 731. (e) Petra, B. *Adv. Mater.* **1998**, *10*, 979.

(2) Touboul, M.; Penin, N.; Nowogrocki, G. *Solid State Sci.* **2003**, *5*, 1327.

(3) (a) Huppertz, H.; von der Eltz, B. *J. Am. Chem. Soc.* **2002**, *124*, 9376. (b) Li, L.; Lu, P.; Wang, Y.; Jin, X.; Li, G.; Wang, Y.; You, L.; Lin, J. *Chem. Mater.* **2002**, *14*, 4963. (c) Emme, H.; Huppertz, H. *Chem.−Eur. J.* **2003**, *9*, 3623. (d) Huppertz, H.; Altmannshofer, S.; Heymann, G. *J. Solid State Chem.* **2003**, *170*, 320. (e) Li, L.; Jin, X.; Li, G.; Wang, Y.; Liao, F.; Yao, G.; Lin, J. *Chem. Mater.* **2003**, *15*, 2253.

(4) (a) Wang, G.-M.; Sun, Y.-Q.; Yang, G.-Y. *J. Solid State Chem.* **2004**, *177*, 4648. (b) Wang, G.-M.; Sun, Y.-Q.; Yang, G.-Y. *J. Solid State Chem.* **2005**, *178*, 729. (c) Liu, G.-Z.; Zheng, S.-T.; Yang, G.-Y. *Inorg. Chem. Commun.* **2007**, *10*, 84. (d) Pan, C.-Y.; Wang, G.-M.; Zheng, S.-T.; Yang, G.-Y. *J. Solid State Chem.* **2007**, *180*, 1553. (e) Pan, C.-Y.; Wang, G.-M.; Zheng, S.-T.; Yang, G.-Y. *Z. Anorg. Allg. Chem.* **2007**, *633*, 336. (f) Yang, S. H.; Li, G. B.; Tian, S. J.; Liao, F. H.; Lin, J. H. *Cryst. Growth Des.* **2007**, *7*, 1246. (g) Visi, M. Z.; Knobler, C. B.; Owen, J. J.; Khan, M. I.; Schubert, D. M. *Cryst. Growth Des.* **2006**, *6*, 538. (h) Wang, M.-S.; Guo, G.-C.; Chen, W.-T.; Xu, G.; Zhou, W.-W.; Wu, K.-J.; Huang, J.-S. *Angew. Chem., Int. Ed.* **2007**, *46*, 3909.

(5) (a) Wang, G.-M.; Sun, Y.-Q.; Yang, G.-Y. *J. Solid State Chem.* **2006**, *179*, 1545. (b) Sung, H. H. Y.; Wu, M.; Williams, I. D. *Inorg. Chem. Commun.* **2000**, *3*, 401. (c) Liu, Z.-H.; Zhang, J.-J.; Zhang, W.-J. *Inorg. Chim. Acta* **2006**, *359*, 519.

10.1021/ic802124v CCC: $40.75
Published on Web 03/12/2009

TM-complex templated borates were usually synthesized under middle-temperature hydrothermal conditions. One of the important applications of borates is based on their optical properties, for example, nonlinear optical (NLO) property.[1e] The most well-known example is the discovery of β-BaB_2O_4 (BBO).[6] BBOs excellent NLO property and wide use in industry rekindled the enthusiasm about the study on borates with NLO activities. Subsequently, some important NLO borate materials, such as LiB_3O_5 (LBO),[7] CsB_3O_5 (CBO),[8] and $Sr_2Be_2B_2O_7$ (SBBO),[9] have also been investigated.

Being in the same group as B, Al can exist in the AlO_4, AlO_5, and AlO_6 forms. Since the discovery of Al in natural zeolites, Al has been used in making numerous artificial zeolites,[10] which have entered into general use in the fields of catalysis, absorption, ion exchange, etc. Besides being used in the synthesis of zeolites, Al was introduced into the borate system by Lehmann et al. giving porous aluminoborates (ABOs) analogous to zeolites.[11] They identified three ABOs with B:Al ratios of 3:1, 2:1, and 2:3, but no further characterization was reported. After that, several ABO phases were revealed.[12] But their structures remain unknown because of the difficulty in synthesizing crystals suitable for structure determination. Recently, Lin et al. synthesized three open-framework ABOs of PKU-1,[13] PKU-5,[14] and PKU-6[15] by using the boric acid flux method. These progresses in the ABO system are stirring; however, no systematic investigation was made on ABOs until now, and the system of ABOs is still weak.

Since 2003, we have made considerable efforts to study hydro(solvo)thermal synthesis of borates and have made great advances in the systems of inorganic,[16] organic,[4a−4e] and TM-complex templated borates.[5a] In order to get open-framework borates, element Ge was introduced into the frameworks of borates successfully by us.[17] As part of our ongoing work, we further extended our interest to make ABOs under hydro(solvo)thermal conditions, which is different from the traditional high-temperature solid-state or boric acid flux synthesis methods. Meanwhile, we chose Al(*i*-PrO)$_3$ (aluminum isopropoxide), not traditional Al_2O_3, $AlCl_3$, or $Al(NO_3)_3$ as an Al source based on the following considerations: (1) the Al(*i*-PrO)$_3$ is easily dissolved in organic solvents, and the chiral Al center may form from three-coordinated Al(*i*-PrO)$_3$ transforming to four-coordinated AlO_4 group via the hydrolysis of Al(*i*-PrO)$_3$ in the crystallization process, and (2) the synergistic combination between chiral AlO_4 groups and acentric B−O clusters formed in situ via self-polymerization of H_3BO_3 will not only greatly increase the likelihood of producing new acentric ABOs, but also offer us the opportunity for choosing efficient NLO materials from these materials. Accordingly, we successfully made a series of open-framework ABOs: $Al[B_5O_{10}]\cdot H_2dab\cdot 2H_2O$ (dab = 1,4-diaminobutane) (**1**), $[Al(B_4O_9)(BO)]\cdot H_2en$ (en = ethylenediamine) (**2**), $[Al(B_4O_9)(BO)]\cdot H_2dap$ (dap = 1,3-diaminopropane) (**3**), $K_2Al[B_5O_{10}]\cdot 4H_2O$ (**4**), and $(NH_4)_2Al[B_5O_{10}]\cdot 4H_2O$ (**5**). Structure **1** is centrosymmetric, whereas **2**−**5** are acentric and present good NLO activities. Although **1** has no NLO property, its framework contains 12-, 11-, and 8-MR intersecting channels and possesses CrB_4 topology.[18]

Experimental Section

Materials and Methods. All chemicals were purchased from commercial sources and used without further purification. Elemental analyses were performed on a Vario EL III elemental analyzer. The FT-IR spectra (KBr pellets) were recorded on an ABB Bomen MB 102 spectrometer. Thermogravimetric analyses were performed on a Mettler TGA/SDTA 851e analyzer with a heating rate of 10 °C min^{-1} under an air atmosphere. XRD powder patterns were collected on a Rigaku DMAX 2500 diffractometer using graphite-monochromated Cu K_α radiation (λ = 1.5418 Å) in the angular range $2\theta = 5-65°$ with a step size of 0.05°. The UV−vis spectra were recorded at room temperature on a computer-controlled PE Lambda 900 UV−vis spectrometer equipped with an integrating sphere in the wavelength range of 190−2000 nm. Fluorescence spectral analyses were performed on a Cary Eclips fluorescence spectrometer. The measurement of the powder frequency-doubling effect was carried out on the unsieved powders of compounds **2**−**5** by means of the Kurtz and Perry method.[19] The fundamental wavelength was 1064 nm and was generated by a Q-switched Nd:YAG laser. The SHG wavelength was 532 nm. KDP powder was used as a reference. ^{27}Al and ^{11}B NMR spectra were recorded on a Varian Infinityplus-400 spectrometer.

Syntheses. Syntheses of the compounds were achieved by a hydrothermal technique in a Teflon-lined stainless steel bomb under synthetic reaction conditions which were determined empirically.

$Al[B_5O_{10}]\cdot H_2dab\cdot 2H_2O$ (1). A mixture of Al(*i*-PrO)$_3$ (0.204 g), H_3BO_3 (0.632 g), dab (0.25 mL), H_2O (1.0 mL), and pyridine (3.0 mL) in a molar ratio of about 1:10:2:37:56 was sealed in a 30 mL stainless reactor with a Teflon liner at 170 °C for 7 days, and then

(6) Chen, C.-T.; Wu, B.-C.; Jiang, A. D.; You, G. M. *Sci. Sin., Ser. B* **1985**, *28*, 235.
(7) Chen, C.; Wu, Y.; Jiang, A.; Wu, B.; You, G.; Li, R.; Lin, S. *J. Opt. Soc. Am. B* **1989**, *6*, 616.
(8) Wu, Y.; Sasaki, T.; Nakai, S.; Yokotani, A.; Tang, H.; Chen, C. *Appl. Phys. Lett.* **1993**, *62*, 2614.
(9) Chen, C.; Wang, Y.; Wu, B.; Wu, K.; Zeng, W.; Yu, L. *Nature* **1995**, *373*, 322.
(10) Baerlocher, C.; Meier, W. M.; Olson, D. H. *Atlas of Zeolite Framework Types*; Elsevier: Amsterdam, The Netherlands, 2001.
(11) Lehmann, H.-A.; Teske, K. *Z. Anorg. Allg. Chem.* **1973**, *400*, 169.
(12) (a) Liu, X.; Xu, R. *J. Chem. Soc., Chem. Commun.* **1989**, 1837. (b) Wang, J.; Feng, S.; Xu, R. *J. Chem. Soc., Chem. Commun.* **1989**, 265. (c) Yu, J.; Xu, R.; Kan, Q.; Xu, Y.; Xu, B. *J. Mater. Chem.* **1993**, *3*, 77. (d) Yu, J.; Chen, J.; Xu, R.; Xu, Y.; Yue, Y. *Polyhedron* **1996**, *15*, 4127. (e) Yu, J.; Xu, R.; Chen, J.; Yue, Y. *J. Mater. Chem.* **1996**, *6*, 465. (f) Yu, J.; Xu, R.; Xu, Y.; Yue, Y. *J. Solid State Chem.* **1996**, *122*, 200. (g) Ayyappan, S.; Rao, C. N. R. *Chem. Commun.* **1997**, 575.
(13) Ju, J.; Lin, J.; Li, G.; Yang, T.; Li, H.; Liao, F.; Loong, C.-K.; You, L. *Angew. Chem., Int. Ed.* **2003**, *42*, 5607.
(14) Ju, J.; Yang, T.; Li, G.; Liao, F.; Wang, Y.; You, L.; Lin, J. *Chem.−Eur. J.* **2004**, *10*, 3901.
(15) Yang, T.; Ju, J.; Li, G.; Liao, F.; Zou, X.; Deng, F.; Chen, L.; Wang, Y.; Lin, J. *Inorg. Chem.* **2007**, *46*, 4772.
(16) (a) Zhang, H.-X.; Zhang, J.; Zheng, S.-T.; Yang, G.-Y. *Inorg. Chem. Commun.* **2004**, *7*, 781. (b) Wang, G.-M.; Sun, Y.-Q.; Yang, G.-Y. *J. Solid State Chem.* **2006**, *179*, 398. (c) Wang, G.-M.; Sun, Y.-Q.; Zheng, S.-T.; Yang, G.-Y. *Z. Anorg. Allg. Chem.* **2006**, *632*, 1586.
(17) (a) Lin, Z. E.; Zhang, J.; Yang, G. Y. *Inorg. Chem.* **2003**, *42*, 1797. (b) Zhang, H. X.; Zhang, J.; Zheng, S. T.; Wang, G. M.; Yang, G. Y. *Inorg. Chem.* **2004**, *43*, 6148. (c) Wang, G. M.; Sun, Y. Q.; Yang, G. Y. *Cryst. Growth Des.* **2005**, *5*, 313. (d) Zhang, H.-X.; Zhang, J.; Zheng, S.-T.; Yang, G.-Y. *Inorg. Chem.* **2005**, *44*, 1166. (e) Pan, C.-Y.; Liu, G.-Z.; Zheng, S.-T.; Yang, G.-Y. *Chem.−Eur. J.* **2008**, *14*, 5057.
(18) O'Keeffe, M.; Eddaoudi, M.; Li, H.; Reineke, T.; Yaghi, O. M. *J. Solid State Chem.* **2000**, *152*, 3.
(19) Kurtz, S. K.; Perry, T. T. *J. Appl. Phys.* **1968**, *39*, 3798.

Table 1. Crystal Data and Structure Refinement for Compounds **1**−**5**

	1	**2**	**3**	**4**	**5**
experimental formula	$C_4H_{18}AlB_5N_2O_{12}$	$C_2H_{10}AlB_5N_2O_{10}$	$C_3H_{12}AlB_5N_2O_{10}$	$H_8AlB_5K_2O_{14}$	$H_{16}AlB_5N_2O_{14}$
formula weight	367.23	303.15	317.18	391.29	349.18
crystal system	monoclinic	monoclinic	monoclinico	Orthorhombic	orthorhombic
space group	$P2_1/c$	Pc	Cc	$C222_1$	$C222_1$
T/K	293	293	293	293	293
λ/Å	0.71073	0.71073	0.71073	0.71073	0.71073
a/Å	8.502(3)	6.6665(4)	10.933(7)	9.340(3)	9.335(4)
b/Å	13.518(5)	8.1507(4)	8.297(5)	10.308(3)	10.487(5)
c/Å	13.914(4)	10.4110(6)	13.317(8)	13.777(5)	14.165(7)
α/°	90	90	90	90	90
β/°	110.9(2)	97.9(1)	97.9(1)	90	90
γ/°	90	90	90	90	90
V/Å^3	1493.8(9)	560.3(5)	1196.5(13)	1326.4(8)	1386.6(11)
Z	4	2	4	4	4
D_c/g cm^{-3}	1.633	1.797	1.761	1.959	1.673
μ/cm^{-1}	0.182	0.234	0.223	0.851	0.221
F (000)	680	308	648	784	720
GOF	1.113	1.052	0.937	1.085	1.165
reflections collected	11425	4222	4488	3836	5366
independent reflections (R_{int})	3396(0.0281)	1863(0.0290)	2395(0.0202)	1490(0.0184)	1577(0.0213)
observed reflections [$I > 2\sigma(I)$]	2752	1699	1981	1429	1536
refined parameters	236	181	200	111	102
R_1/wR_2 [$I > 2\sigma(I)$]	0.0368/0.1053	0.0357/0.0814	0.0384/0.0912	0.0249/0.0732	0.0319/0.0960
R_1/wR_2 (all data)	0.0467/0.1184	0.0407/0.0843	0.0478/0.0982	0.0259/0.0736	0.0326/0.0965

cooled to room temperature. Colorless needle-like crystals of **1** were recovered by filtration, washed with distilled water, and dried in air, respectively. Yield: 65% (based on Al). Anal. Calcd for **1**: C, 13.08; H, 4.94; N, 7.63%. Found: C, 13.02; H, 4.75; N, 7.58%.

IR bands (cm^{-1}) for **1**: 3475m, 3091w, 2942w, 1449s, 1292s, 1235s, 1080m, 1045m, 970m, 940m, 871m, 726m, 685m, 657w, 624w, 508w, 485w, and 423w.

[Al(B$_4$O$_9$)(BO)]·H$_2$en (2). In a typical synthesis for **2**, a mixture of Al(*i*-PrO)$_3$ (0.204 g) and H_3BO_3 (0.376 g) was dispersed in a mixture of H_2O (1.0 mL) and pyridine (3.0 mL) and was stirred to a homogeneous gel. Then ethylenediamine (1.0 mL) was added to the gel. The mixture with the composition of Al(*i*-PrO)$_3$/H_3BO_3/en/pyridine/H_2O in a molar ratio of 1:6:15:37:56 was transferred to a 23 mL Teflon-lined stainless steel bomb and was heated at 170 °C for 7 days. Colorless needle-like crystals were obtained by sonication, and the crystals were washed with distilled water and then dried in air. The yield was about 85% (based on Al). Anal. Calcd for **2**: C, 7.67; H, 3.52; N, 9.20%. Found: C, 7.92; H, 3.32; N, 9.24%. IR bands (cm^{-1}): 3227w, 3127w, 2972w, 2915w, 1601w, 1324s, 1198m, 1080m, 940m, 857w, 838w, 766m, 706w, 629m, 580w, and 428w.

[Al(B$_4$O$_9$)(BO)]·H$_2$dap (3). A mixture of Al(*i*-PrO)$_3$ (0.204 g), H_3BO_3(0.804 g), dap (0.3 mL), H_2O (1.0 mL), and pyridine (3.0 mL) in a molar ratio of 1:13:4:37:56 was reacted in a 30 mL Teflon-lined stainless steel bomb at 170 °C for 7 days and then cooled to room temperature. Colorless needle-like crystals suitable for X-ray diffraction were obtained in 81% yield (based on Al). Anal. Calcd for **3**: C, 11.01; H, 3.89; N, 8.83%. Found: C, 11.86, H, 3.81; N, 8.83%. IR bands (cm^{-1}): 3420w, 3244w, 2976w, 2917w, 1633s, 1360s, 1190w, 1101m, 1045w, 953m, 923m, 856w, 833w, 761m, 703w, 626m, 587m, and 510w.

K$_2$Al[B$_5$O$_{10}$]·4H$_2$O (4). A mixture of Al(*i*-PrO)$_3$ (0.204 g), $K_2B_4O_7$·4H_2O (0.611 g), H_2O (1.0 mL), and pyridine (3.0 mL) in a molar ratio of about 1:2:37:56 was sealed in a 30 mL Teflon-lined stainless steel bomb, heated at 170 °C for 7 days, and then cooled to room temperature. Prismatic crytals of **4** were obtained. Yield: nearly 100% (based on Al). IR bands (cm^{-1}) for **4**: 3612w, 3533s, 2359w, 1632w, 1377s, 1309s, 1247s, 1084m, 1064m, 948s, 866m, 729m, 709m, 664w, 583w, 560w, 493m, and 438w.

(NH$_4$)$_2$Al[B$_5$O$_{10}$]·4H$_2$O (5). A mixture of Al(*i*-PrO)$_3$ (0.204 g), H_3BO_3 (0.811 g), $CO(NH_2)_2$ (0.847 g), H_2O (1.0 mL), and pyridine (3.0 mL) in a molar ratio of about 1:13:14:37:56 was sealed in a 30 mL Teflon-lined stainless steel bomb, heated at 170 °C for 7 days, and then cooled to room temperature. Prismatic crytals of **5** were obtained. Yield: 40% (based on Al). Anal. Calcd for **5**: H, 4.58; N, 8.00%. Found: H, 4.58; N, 7.87%. IR bands (cm^{-1}) for **5**: 3626w, 3426m, 3228m, 2345w, 1650w, 1454s, 1372s, 1303s, 1241s, 1056m, 946s, 852m, 700s, 584w, 560w, 490w, and 431w.

Single-Crystal Structure Determination. The intensity data sets were collected on a Rigaku Mercury CCD (**1**, **2**) or a Rigaku Saturn70 CCD (**3**−**5**) with graphite-monochromated Mo Kα radiation (λ = 0.71073 Å) in the ω scanning mode at room temperature. All absorption corrections were performed using the multiscan program. The structures were solved by direct methods and refined by full-matrix least-squares on F^2 with the SHELXTL-97 program.[20] The H-atoms of the organic ligands were geometrically placed and refined using a riding model. However, the H-atoms of the water molecules in compound **4** have not been included in the final refinement. All atoms except for H-atoms were refined anisotropically. Further details for the structural analyses of **1**−**5** are summarized in Table 1, and the selected bond lengths of compounds **1**−**5** are listed in Table 2. The purities of the compounds were confirmed by XRD powder diffraction studies (Figure 1). The CCDC reference numbers for the compounds are 693069 (**1**), 675161 (**2**), and 675162 (**3**), and the ICSD numbers are 419868 (**4**) and 419867 (**5**).

Computational Description. The band structures and density of states (DOS) of anionic frameworks for compounds **1**−**5** were theoretically calculated by using the computer code CASTEP.[21] The total energy is calculated with the density functional theory (DFT) using the Perdew−Burke−Ernzerhof generalized gradient approximation (GGA).[22] The following orbital electrons are treated as valence electrons: Al 3s^{2}3p^1, B 2s^{2}2p^1, and O 2s^{2}2p^4. The number of plane waves included in the basis is determined by a cutoff energy of 300 eV, and the numerical integration of the Brillouin zone is performed using a Monkhorst−Pack k point sampling: 3 × 1 × 2 for **1**, 3 × 2 × 2 for **2**, 3 × 3 × 2 for **3**, and 3 × 3 × 1 for

(20) (a) Sheldrick, G. M. *SHELXS-97, Program for Solution of Crystal Structures*; University of Göttingen: Germany, 1997. (b) Sheldrick, G. M. *SHELXS-97, Program for Solution of Crystal Refinement*; University of Göttingen: Germany, 1997.

Table 2. Selected Bond Distances for Compounds **1**−**5**[a]

compound **1**		compound **2**		compound **3**		compound **4**		compound **5**	
Al−O(4)#1	1.719(1)	Al−O(4)#4	1.714(2)	Al−O(1)#7	1.703(2)	Al−O(4)#10	1.733(2)	Al−O(5)#14	1.734(1)
Al−O(3)#2	1.735(1)	Al−O(1)#5	1.721(2)	Al−O(4)#8	1.706(2)	Al−O(4)	1.733(2)	Al−O(5)#8	1.734(1)
Al−O(2)#3	1.737(1)	Al−O(9)	1.753(2)	Al−O(9)	1.740(2)	Al−O(5)#11	1.743(1)	Al−O(4)#15	1.741(1)
Al−O(1)	1.749(1)	Al−O(10)	1.770(2)	Al−O(10)	1.780(2)	Al−O(5)#12	1.743(1)	Al−O(4)	1.741(1)
B(1)−O(1)	1.347(2)	B(1)−O(2)	1.367(4)	B(2)−O(7)	1.431(4)	B(1)−O(4)	1.342(2)	B(1)−O(4)	1.340(2)
B(1)−O(7)	1.350(2)	B(1)−O(1)	1.367(4)	B(2)−O(2)	1.467(4)	B(1)−O(3)	1.357(2)	B(1)−O(3)	1.359(2)
B(1)−O(5)	1.388(2)	B(1)−O(6)	1.372(4)	B(2)−O(3)	1.479(4)	B(1)−O(1)	1.397(3)	B(1)−O(1)	1.391(2)
B(2)−O(2)	1.343(2)	B(2)−O(7)	1.440(3)	B(2)−O(10)	1.524(3)	B(2)−O(5)	1.341(2)	B(2)−O(5)	1.337(2)
B(2)−O(6)	1.369(2)	B(2)−O(2)	1.465(4)	B(1)−O(1)	1.340(4)	B(2)−O(2)	1.357(2)	B(2)−O(2)	1.360(2)
B(2)−O(5)	1.383(2)	B(2)−O(3)	1.472(4)	B(1)−O(2)	1.366(4)	B(2)−O(1)	1.394(2)	B(2)−O(1)	1.387(2)
B(3)−O(7)	1.461(2)	B(2)−O(10)	1.530(4)	B(1)−O(6)	1.373(4)	B(3)−O(3)#13	1.458(2)	B(3)−O(2)	1.470(2)
B(3)−O(10)	1.465(2)	B(3)−O(4)	1.353(4)	B(4)−O(8)	1.449(3)	B(3)−O(3)	1.458(2)	B(3)−O(2)#16	1.470(2)
B(3)−O(6)	1.477(2)	B(3)−O(5)	1.367(4)	B(4)−O(5)	1.463(3)	B(3)−O(2)#13	1.476(2)	B(3)−O(3)	1.473(2)
B(3)−O(8)	1.480(2)	B(3)−O(3)	1.381(4)	B(4)−O(6)	1.473(3)	B(3)−O(2)	1.476(2)	B(3)−O(3)#16	1.473(2)
B(4)−O(4)	1.336(2)	B(4)−O(8)	1.449(4)	B(4)−O(10)	1.506(3)				
B(4)−O(10)	1.359(2)	B(4)−O(6)	1.456(4)	B(3)−O(4)	1.342(4)				
B(4)−O(9)	1.406(2)	B(4)−O(5)	1.468(4)	B(3)−O(3)	1.372(4)				
B(5)−O(3)	1.338(2)	B(4)−O(10)	1.523(3)	B(3)−O(5)	1.376(3)				
B(5)−O(8)	1.364(2)	B(5)−O(9)	1.348(4)	B(5)−O(9)	1.343(4)				
B(5)−O(9)	1.396(2)	B(5)−O(7)	1.375(4)	B(5)−O(7)	1.360(4)				
		B(5)−O(8)#6	1.376(3)	B(5)−O(8)#9	1.384(4)				

[a] Symmetry codes: #1, $x-1,y,z$; #2, $-x,y+1/2,-z+1/2$; #3, $x,-y+1/2,z+1/2$; #4, $x,-y+1,z-1/2$; #5, $x,-y+2,z-1/2$; #6, $x+1,y,z$; #7, $x-1/2,y+1/2,z$; #8, $x-1/2,y-1/2,z$; #9, $x,-y+1,z+1/2$; #10, $x,-y+1,-z+1$; #11, $x-1/2,y+1/2,z$; #12, $x-1/2,-y+1/2,-z+1$; #13, $-x,y,-z+1/2$; #14, $x-1/2,-y+1/2,-z+3$; #15, $x,-y,-z+3$; #16, $-x+1,y,-z+5/2$.

4 and **5**. The other calculating parameters and convergent criteria were the default values of the CASTEP code.

Results and Discussion

Structure of 1. Single-crystal X-ray analysis indicates the asymmetric unit of compound **1** contains 24 independent non-H-atoms, including 1 Al, 2 N, 4 C, 5 B, and 12 O (see Supporting Information, Figure S1). All atoms are located in general positions. The B atoms reveal two kinds of coordination models with B−O bond distances varying from 1.336(2) to 1.406(2) Å for the BO_3 triangles and 1.461(2) to 1.480(2) Å for the BO_4 tetrahedra. The O−B−O bond angles are distributed in the range of 117.5(1)−124.1(2)° for the triangles and 108.1(1)−111.8(1)° for the tetrahedra. The Al atom adopts tetrahedral coordination with Al−O bond distances varying from 1.719(13) to 1.749(13) Å and O−Al−O angles changing from 105.2(1) to 113.2(1)°. All O atoms are bridged by B or Al centers. Four BO_3 triangles and one BO_4 tetrahedron are polymerized into a B_5O_{10} cluster with four potential coordination O atoms, in which two B_2O_3 rings are perpendicularly linked by a common BO_4 tetrahedron. In crystalline borates such an arrangement of B centers is commonly observed in the isolated $[B_5O_6(OH)_4]^{2-}$ anion, in which four terminal hydroxyl ligands prevent further connection of $[B_5O_6(OH)_4]^{2-}$.[4b,g,5a,c]

The overall 3D anionic framework of **1** is built up from strictly alternating B_5O_{10} clusters and AlO_4 tetrahedra. There is no Al−O−Al connection. Each B_5O_{10} cluster is connected to 11 others through four bridging AlO_4 groups (Figure 2a), and each AlO_4 group is also connected to 11 others through four bridging B_5O_{10} clusters (Figure 2b). The alternating connection of the AlO_4 tetrahedra and B_5O_{10} clusters through O(3,4) bridges leads to a helical chain along the *b* axis. The left- and right-handed helical chains are alternately connected by common O2 atoms to form an infinite layer with 12- and 8-MR openings parallel to the (100) plane. Along the *a* axis these layers are further bridged by the O4 atoms, resulting in the formation of the final 3D framework with 3D intersecting channels. Along the [100] direction, two parallel channels co-exist (Figure 2c): the elliptical 12-MR channels with a free-pore diameter of 4.0 × 6.3 Å (assuming van der Waals diameter of oxygen is 2.7 Å) (see Supporting Information, Figure S2) built from four AlO_4 and eight BO_3 units containing two repeating $-AlO_4-B1O_3-B2O_3-AlO4-B4O_3-B5O_3-$ linkages, and the 8 MR channels with a free-pore diameter of 1.3 × 4.1 Å (see Supporting Information, Figure S2) bound by two AlO_4, two BO_4, and four BO_3 units in the two repeating linkage of $-AlO_4-B5O_3-B3O_4-B2O_3-$. Each 12-MR channel is surrounded by four 8-MR channels and vice versa. Interestingly, the two kinds of channels are filled with a different amount of guest species according to their pore size (see Supporting Information, Figure S2). The 12-MR channels are occupied by one H_2dab cation and two free water molecules, while the 8-MR channels are only filled with another unique H_2dab cation and no water molecules are found. Moreover, the water molecules are found near the walls of the 12-MR channels. A similar phenomenon has been observed in ND-1.[23] There are strong hydrogen bonds

(21) (a) Segall, M. D.; Lindan, P. J. D.; Probert, M. J.; Pickard, C. J.; Hasnip, P. J.; Clark, S. J.; Payne, M. C. *J. Phys.: Condens. Matter* **2002**, *14*, 2717. (b) Milman, V.; Winkler, B.; White, J. A.; Pickard, C. J.; Payne, M. C.; Akhmatskaya, E. V.; Nobes, R. H. *Int. J. Quantum Chem.* **2000**, *77*, 895.

(22) Perdew, J. P.; Burke, K.; Ernzerhof, M. *Phys. Rev. Lett.* **1996**, *77*, 3865.

(23) Yang, G. Y.; Sevov, S. C. *J. Am. Chem. Soc.* **1999**, *121*, 8389.

(24) During testing of NLO properties for a series of ABOs with acentric structures, two ABOs were reported, i.e. $(TETA)_2[Al_2(B_{10}O_{20})]\cdot 0.25H_2O$, ref 24a, and $[CH_3NH_2(CH_2)_3]$- $[AlB_5O_{10}]$, ref 24b, which are the members of our series of ABOs templated by organic amines. See also: (a) Wang, G.-M.; Li, J.; Li, Z.; Huang, H.; Xue, S.; Liu, H. *Inorg. Chem.* **2008**, *47*, 1270. (b) Wang, G.-M.; Li, J.; Huang, H.; Li, H.; Zhang, J. *Inorg. Chem.* **2008**, *47*, 5039.

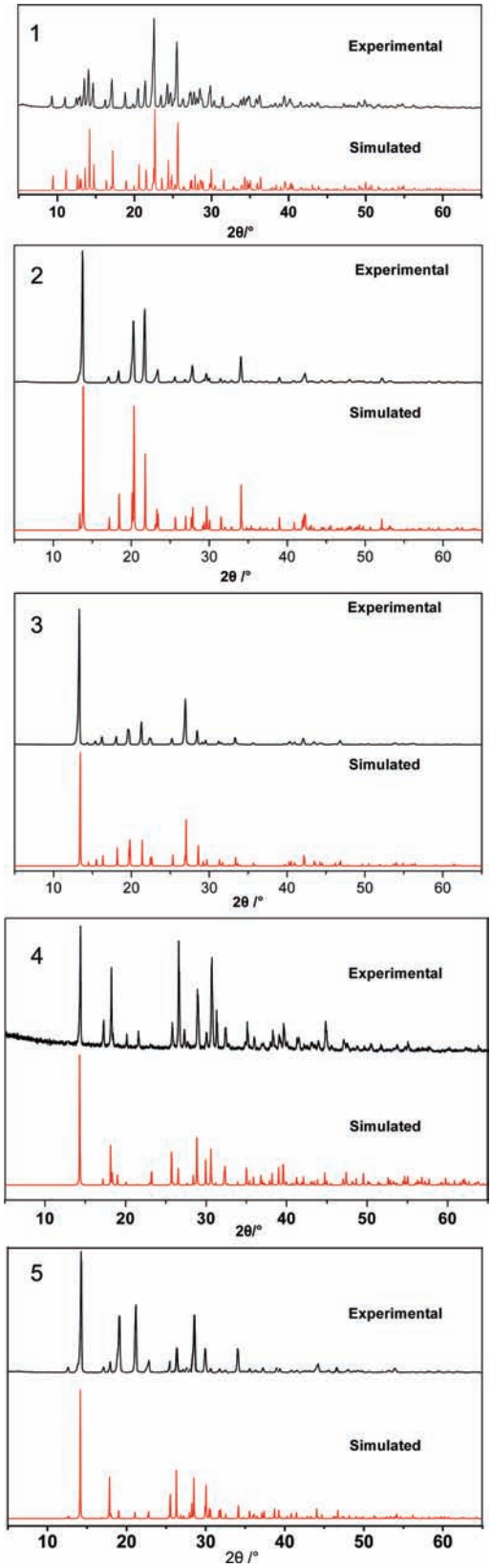

Figure 1. Simulated and experimental powder XRD patterns of **1**−**5**.

between the guest molecules and the framework with O−H···O distances in the range of 2.833(2)−3.254 (2) Åand N−H···O distances in the range of 2.723(3)−3.337(8) Å.

It is worth noting that the framework possesses partially overlapped odd 11-ring channels in the [010], [101], and

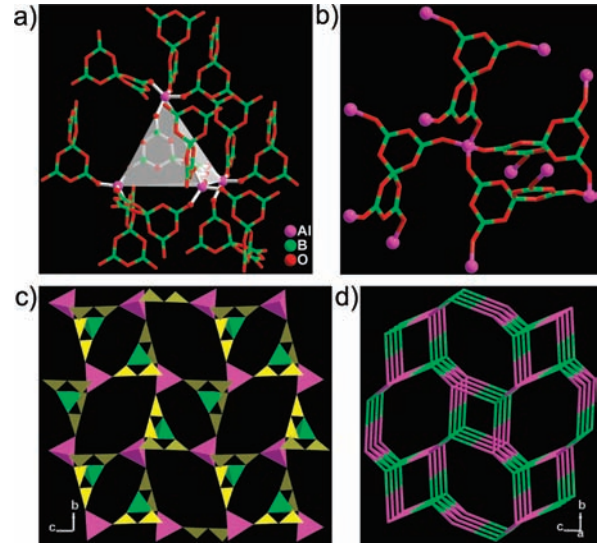

Figure 2. (a,b) Views of the linkage of B_5O_{10} and AlO_4 groups in **1**. Each B_5O_{10}/AlO_4 unit is bridged by four AlO_4/B_5O_{10} groups to 11 other B_5O_{10}/AlO_4 units. (c) The open-framework structure of **1** along the *a* axis showing the 12- and 8-MR channels. The organic amine cations and free water molecules have been omitted for clarity. Color code: AlO_4 is pink, BO_4 is green, BO_3 is yellow and similarly hereinafter. (d) Topology of **1** is the same as that of CrB_4 with vertex symbols $4{\cdot}6_2{\cdot}6{\cdot}6{\cdot}6{\cdot}6$.

[110] directions (see Supporting Information, Figure S2). Among the known crystallized ABOs, the odd 11-ring channels are rare and only found in QD-2[24a] and QD-3,[24b] which prolongate in one direction. The structure of **1** presents the first example of ABOs with odd 11-ring channels in the three directions. The windows of the 11-ring channels are delimited by three AlO_4, two BO_4, and six BO_3. From the topological point of view, the 3D framework of **1** has the same topology as CrB_4 and FJ-18[17e] with a vertex symbol of $4{\cdot}6_2{\cdot}6{\cdot}6{\cdot}6{\cdot}6$ (Figure 2d), in which both B_5O_{10} and AlO_4 units act as four-connected nodes.

Structures of 2 and 3. The asymmetric unit of **2** contains an Al atom, a BO group, and a B_4O_9 unit comprising two BO_3 triangles (□) and two BO_4 tetrahedra (T) (described as 4:2□ + 2T according to the classification scheme of Christ and Clark[1a]). The acentric B_4O_9 unit containing two chiral centers (B2 and B4) is linked by an acentric BO_3 triangle via a μ_2-O7 atom to form an unusual acentric $[B_4O_9(BO_2)]$ unit (5:[4:(2□ + 2T) + (1□)]) (Figure 3a) that differs from the known B_5O_{11} unit (5:3□ + 2T).[25] The acentric $[B_4O_9(BO_2)]$ unit chelates a chiral tetrahedral Al center through μ_2-O9 and μ_3-O10 atoms, forming a novel acentric AlB_5O_{13} cluster with three chiral centers (B2, B4, and Al) and three 3-MRs. In the chiral AlO_4 group, the O1A and O4B atoms are linked to two other AlB_5O_{13} clusters, respectively. Thus, each AlB_5O_{13} cluster links six others via six μ_2-O (two O1, two O4, and two O8) atoms (Figure 3b).

As shown in Figure 3a, only the O10 atom is three coordinate and joins one AlO_4 and two BO_4 tetrahedra while other O atoms are two coordinate. As expected, the distance of the μ_3-O−B bond (av 1.526(8) Å) is longer than that of the μ_2-O−B bonds (av 1.403 (9) Å). Compared with the AlB_5O_{13} cluster in **2**, the analogous μ_3-O atoms are also

(25) Tu, J. M.; Keszler, D. A. *Inorg. Chem.* **1996**, *35*, 463.

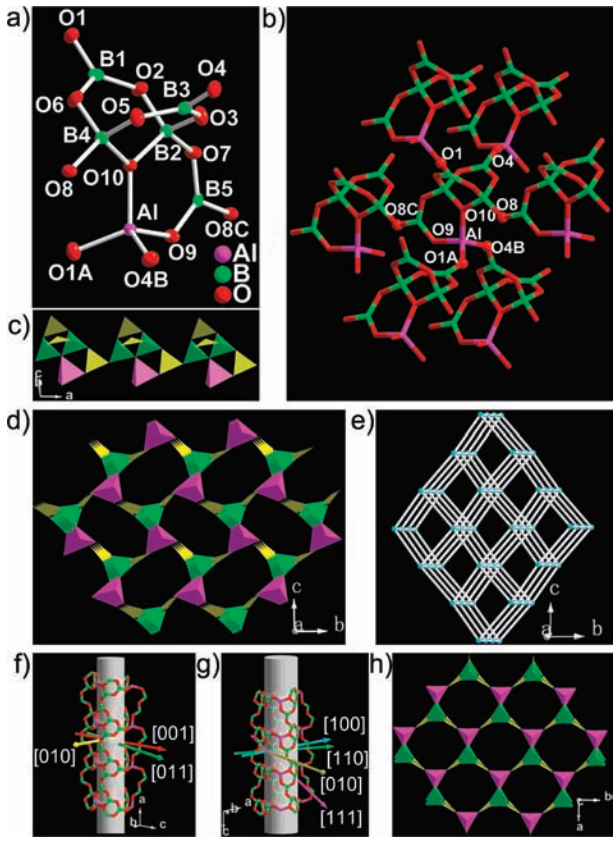

Figure 3. (a) ORTEP view of the AlB_5O_{13} cluster in **2**. (b) View of the linking mode of the AlB_5O_{13} SBU, showing that each AlB_5O_{13} links six others. (c) A view of the AlB_5O_{13} chain along the *a* axis. (d) View of the 10-MR channels in **2** along the *a* axis. (e) View of the 6-connected 3D topology network in **2**. Color code: AlB_5O_{13} node is cyan. (f) View of three pairs of 9-MR windows intersecting with the 10-MR channel in **2** along the [010], [001], and [011] directions shown as yellow, red, and green arrows, respectively. (g) View of four pairs of 9-MR windows intersecting with the 10-MR channels in **3** along the [100], [010], [110], and [111] directions shown as cyan, yellow, green, and pink arrows, respectively. (h) View of the 10-MR channels in **3** along the *c* axis.

observed in the reported B_6O_{13} cluster (6:3□ + 3T),[26] in which the μ_3-O atoms join three BO_4 units. Therefore, the AlB_5O_{13} cluster can be considered as the transfiguration of the centrosymmetric B_6O_{13} cluster: substituting a BO_4 group of the B_6O_{13} cluster with an AlO_4 group, and then one BO_3 triangle is transplanted to link two BO_4 groups by corner-sharing, forming the acentric AlB_5O_{13} cluster (see Supporting Information, Figure S3). The AlB_5O_{13} clusters being SBUs link to each other via O8 atoms to form a $\{AlB_5O_{13}\}_n$ chain along the *a* axis (Figure 3c). Each chain is further connected by an adjacent four others via two O1 and two O4 atoms to form a novel open framework with 3D intersecting 10-, 9-, 9-, and 9-MR channels along the [100] (Figure 3d), [010], [001], and [011] directions, respectively. The H_2en cations are housed in 10-MR channels and interact with the walls of the channels through H-bonds with an average N−H···O distance of 2.943(6) Å (see Supporting Information, Figure S4). From the topological point of view, the 3D framework of **2** is a six-connected network if each AlB_5O_{13} SBU acts as a six-connected node. The network is shown schematically in Figure 3e, and its Schäfli symbol is $4^{12}6^3$. Along the *a* axis, the 10-MR windows are rectangle-like and consist of three AlO_4, three BO_4, and four BO_3 groups in AlO_4−BO_3−BO_4−AlO_4−BO_3−BO_4−BO_3−AlO_4−BO_4−BO_3 linkages with the dimensions of 2.3 × 5.6 Å (see Supporting Information, Figure S4). Three 9-MRs along the [010], [001], and [011] directions intersect with 10-MR channels along the *a* axis to form six 9-MR windows perpendicular to the 10-ring channel (Figure 3f). Although the shapes of three 9-MR windows that run along the [010], [001], and [011] directions are different, the atomic arrangements are similar. They are built from two AlO_4, three BO_4, and four BO_3 groups in the linkages of AlO_4−BO_3−BO_4−BO_3−BO_4−BO_3−AlO_4−BO_4−BO_3. Therefore, **2** contains a 3D-intersecting channel system in which all the channels can directly communicate with each other (see Supporting Information, Figure S5).

As for **3**, it contains similar SBUs, the AlB_5O_{13} clusters. Each SBU is linked to six others by six μ_2-O (two O1, two O4, two O8) atoms, resulting in an open framework with a 3D-intersecting channel system containing 10-, 9-, 9-, 9-, and 9-MR along the [001], [100], [010], [110], and [111] directions, respectively (Figure 3g). Different from the rectangle-like 10-MR channels in **2** in which the H_2dap cations are located, the 10-MR channels in **3** are square-like (Figure 3h) with the dimensions of 4.1 × 4.1 Å (see Supporting Information, Figure S6). Though **2** and **3** possess similar SBUs and linkages between $[B_4O_9(BO)]$ clusters and AlO_4 groups in the structures, they reveal two different acentric open frameworks with distinct shapes of the 10-MR channels and different 3D-intersecting channel systems because of different structure-directing agents (SDAs).

Structures of 4 and 5. Compounds **4** and **5** are isomorphous; therefore, only the structure of **4** will be represented. The asymmetric unit of **4** contains one Al in a two-fold axis that is four-coordinated. B1 and B2 in general positions are three-coordinated. B3 are four-coordinated in a two-fold screw axis. Two BO_3 groups join each other through a μ_2-O atom to form two B_2O_5 dimers that are further linked by a BO_4 group, forming a B_5O_{10} unit comprised of two 3-MRs; the B_5O_{10} joins four AlO_4 groups by four μ_2-O atoms and vice versa. Different from compound **1**, each B_5O_{10} cluster is connected to 12 others through four bridging AlO_4 groups and vice versa (Figure 4a,b), resulting in no Al−O−Al connection in **4**. The alternate connection between B_5O_{10} and AlO_4 through their vertices gives rise to a 3D macroanionic $[Al(B_5O_{10})]_n^{2n-}$ framework with an intersecting channel system containing 11-, 11-, 8-, 8-, and 8-MR channels along the [110] (Figure 4c), [−110], [100], [010], and [001] directions (see Supporting Information, Figure S7), respectively, in which all the 8-MR channels are helical and built by two AlO_4 and two B_5O_{10} clusters via alternate connections: the right-handed helices for the *a* axis and the left-handed helices for the *b*/*c* axis (Figure 4d). The K^+ cations and free H_2O molecules sit at the 11-MR channels. The odd 11-MR channels with the dimensions of 2.7 × 6.7 Å are made of three AlO_4, two BO_4, and six BO_3 groups in the linkages of AlO_4−BO_3−BO_4−BO_3−AlO_4−BO_3−BO_3−

(26) Touboul, M.; Penin, N.; Nowogrocki, G. *J. Solid State Chem.* **2000**, *150*, 342.

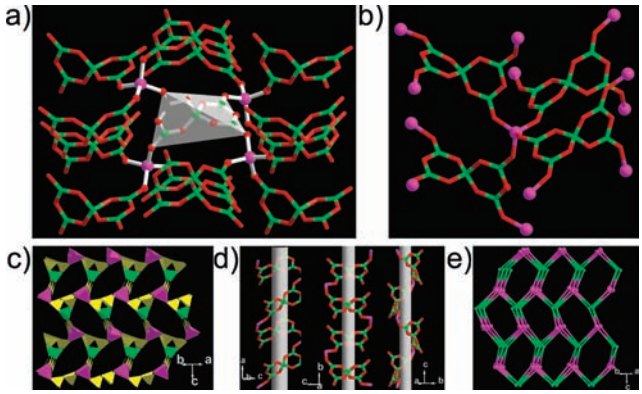

Figure 4. (a,b) Views of the linkage of B_5O_{10} and AlO_4 groups in **4** and **5**. Each B_5O_{10}/AlO_4 unit is bridged by four AlO_4/B_5O_{10} groups to 12 other B_5O_{10}/AlO_4 units. (c) View of the 11-MR channels in **3** along the [110] direction. (d) View of three helical 8-MR channels, showing the right-, left-, and left-handed character along the [100], [010], and [001] directions, respectively. (e) Topological view of the network along the [110] direction. Color codes: AlO_4 is pink nodes and B_5O_{10} is green nodes.

$AlO_4-BO_3-BO_4-BO_3$. All the channels can also communicate to each other. From the topological point of view, the 3D framework of **4** is a four-connected network if each AlO_4 group and each B_5O_{10} SBU acts as a four-connected node. The network is shown schematically in Figure 4e, and its Schäfli symbol is 6^6. Compound **5** has the same framework as **4**. The NH_4^+ cations and H_2O molecules are guests in the 11-MR channels. The NH_4^+ cation is bonded to three different O(1,2,5)-atoms of the framework through two H(1,3)-atoms and two H_2O molecules (OW2, OW3) through the other H(2,4)-atoms with a N···O distance of 2.921(3)−3.039(2) Å. All the H_2O molecules are H-bonded to the framework, and there are intermolecular H-bonds between OW1 and OW2 with an O···O distance of 2.773(2)−3.054(2) Å (see Supporting Information, Figure S7). For **4** and **5**, the difference is only in the cations, and the unit cell volume of **5** (1386.6(11) $Å^3$) is larger than those of **4** (1326.4(8) $Å^3$), which indicates the NH_4^+ ion is larger than K^+ ion. Though the value of the *a* axis (9.335(4) and 9.340(3) Å for **5** and **4**) is similar, the unit cell parameters *b* and *c* for **5** (10.487(5)/14.165 (7) Å) are larger than that of **4** (10.308(3)/13.777(5) Å). Therefore, the considerable anisotropic change with respect to the three unit cell axes for **5** might be associated with the anisotropic hydrogen bonds in the compound **5**.

Discussion

As we have mentioned, in contrast to compound **1**, compounds **2** and **3** are acentric structures and **4** and **5** are chiral structures. In **1**, the central symmetry of dab transfers to the framework through a strong templating effect. Notice that the acentric B−O clusters in **2** and **3** govern the acentric characteristic of the Al−B−O host frameworks, even if the centrosymmetric amines, en and dap, were used as SDAs in **2** and **3**, respectively. To our knowledge, the en often demonstrates a strong templating effect, but it does not govern the acentric characteristic of the framework of **2**. In **2** and **3** not only does the acentric characteristic of the B−O clusters transfer to Al−B−O frameworks, but the combination between chiral AlO_4 groups and acentric B−O clusters also results in the acentric characteristic of Al−B−O frameworks while the centrosymmetric SDAs in **2** and **3** only show weak templating effects and do not govern the acentricity of the Al−B−O frameworks through hydrogen-bonding interactions. This is because the acentric AlB_5O_{13} clusters in **2** and **3** are connected by covalent Al−O−B bonds and further transmit their acentric characteristic to the Al−B−O frameworks through the stronger Al−O−B covalent interactions. In **4** and **5**, the acentric B_5O_{10} cluster governs the acentricity of the frameworks.

Generally two factors, the SDAs and the chiral/acentric inorganic groups, will impact the chirality and acentricity of the inorganic frameworks. According to the principle of the host−guest symmetry matching, the chiral/acentric amines, such as SDAs, impart their chirality or acentricity into the host inorganic frameworks, and many chiral/acentric materials are made. In this case, the chiral/acentric SDAs govern the chirality/acentricity of the frameworks. However, the centrosymmetric SDAs, such as en, also govern the characteristic of the frameworks, resulting in not only the centrosymmetric frameworks (**FJ-18**[17e]) but also the chiral materials (ICMM6[27]). This is because the syntheses of the chiral/acentric materials involving complex reaction mechanisms are poorly understood so far. The chiral/acentric SDAs are just one of the important factors for making chiral/acentric materials. As to chiral/acentric B−O cluster groups, they not only transfer their chiral/acentric characteristic to inorganic frameworks, but they also govern the chiral/acentric characteristic of the frameworks, such as **2**−**5**.

NLO, UV−Vis and Fluorescence Spectra Determination. Considering the noncentrosymmetric structures of **2**−**5**, the second harmonic generation (SHG) measurements are carried out on the powder samples of these compounds by the Kurtz−Perry method[19] at room temperature. The intensity of the green light (frequency-doubled output: $\lambda =$ 532 nm) produced by the crystal powder of these compounds exhibits a SHG efficiency of about 1.9, 2.1, 2.0, and 2.0 times higher than that of KDP (KH_2PO_4) powder, respectively. In addition, the SHG signals not only reveal that compounds **2**−**5** have a powder SHG effect better than that of KDP powder, but the SHG signals also provide a highly sensitive and definitive test for the absence of a center of symmetry.

The UV−vis absorption spectral measurements indicate that **2** and **3** are transparent in the range of 400−2000 nm, but near-infrared absorption of H_2O molecules is presented in the spectra for **1**, **4**, and **5**. From 400 to 190 nm, the absorptions increase with the decreasing wavelength, and the largest absorption rates are about 10.0, 11.5, 10.9, 8.9, and 13.1% at 193 nm for **1**−**5**, respectively (see Supporting Information, Figure S8). According to the Kubelka−Munk function where $\alpha/S = (1-R)^2/2R$, optical diffuse reflectance studies reveal that the band gaps of **1**−**5** are ca. 3.67, 4.11, 4.23, 4.45, and 3.96 eV (Figure 5), showing that **1**−**5** are wide-band-gap semiconductors.

(27) Medina, M. E.; Iglesias, M.; Snejko, N.; Gutierrez-Puebla, E.; Monge, M. A. *Chem. Mater.* **2004**, *16*, 594.

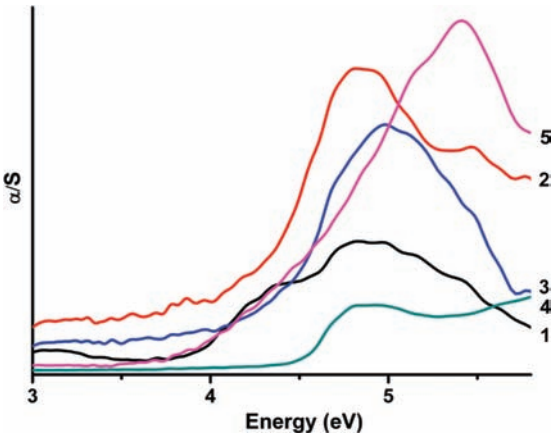

Figure 5. UV−vis optical diffuse reflectance spectra for compounds **1**−**5**.

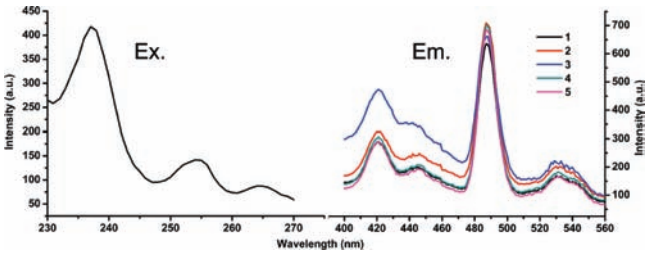

Figure 6. Excitation and emission spectra of compounds **1**−**5**.

The five compounds all have the strongest blue luminence emission at 487 nm as a result of excitation by 237 nm wavelength. The emission and excitation spectra are shown in Figure 6. Although the five compounds contain different organic or inorganic cations in their channels, emission spectra shows they have almost the same emission intensity at 487 nm, which probably means the fluorescence emission of the five compounds is not relevent to the template cations.

Theoretical Studies. The measured results of the UV−vis and fluorescence spectra showed identical optical properties for the five compounds. So, we conjecture the frameworks of the five compounds have similar energy band structures. To demonstrate this, we calculate the energy band structures and density of states (DOS) of the frameworks for the five compounds based on the DFT method by using the computer code CASTEP. The calculated results confirmed our theory. It is found that the five compounds have similar energy bond structure (see Supporting Information, Figure S9) and DOS (Figure 7a). Their valence bonds (VBs) are almost flat, and conduction bonds (CBs) display a small dispersion. Their state energies of the lowest-conduction bonds (L-CB) and the highest-valence bonds (H-VB) are located in the same high symmetry point, respectively. Therefore, they are all direct band gap semiconductors with band gaps of 5.40, 5.32, 5.31, 5.45, and 5.44 eV, which are bigger than the experimental band gaps and correspond to the UV absorption of about 230 nm. Their bands can be assigned according to total and partial DOS (Figure 7b). Taking the compound **1** for example, the VBs from −20.0 to −16.0 are mainly contributions of O-2s states. The bands

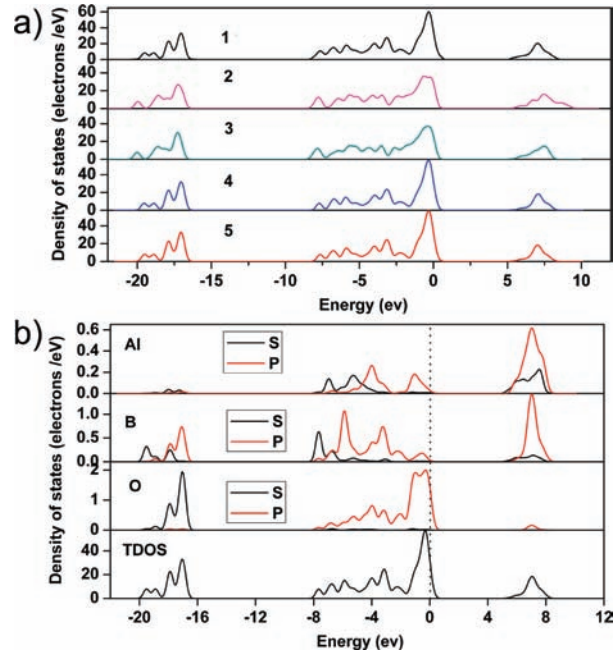

Figure 7. (a) Density of states for compounds **1**−**5**. (b) The partial and total density of states.

from −8 eV to the Fermi level are mainly derived from O-2p and B-2p states. The CBs are dominated by unoccupied Al-3p and B-2p states.

Thermal Stability Analysis. To study the thermal stability of compounds **1**−**5**, thermogravimetric analyses (TGA) in air at a heating rate of 10 °C min^{-1} were performed on polycrystalline samples to determine their thermal stabilities (see Supporting Information, Figure S10). For **1**, the total loss of 9.50% weight in the first step from 30 to 162 °C corresponds to the release of two free water molecules (calcd: 9.80%). Above 290 °C, a gradual weight loss of 23.93% up to 1000 °C was observed and assigned to the removal of the dab molecules (calcd: 23.96%). Compounds **2** and **3** are stable to 380 and 360 °C, respectively. Subsequently, the TG curves show that the guest molecules were gradually lost until 878 °C for **1** (calcd: 25, found: 25.5%) and for **2** (calcd: 29.1, found: 29.2%). For **4**, the TG curve shows a weight loss of about 18.3% in the range from 32 to 216 °C, which is in good agreement with the theoretical value of 18.4%, corresponding to the removal of the guest water molecules. The TG curve for **5** shows the compound is stable up to 307 °C, and then a continuous weight loss occurs between 307 and 530 °C (calcd: 35.5, found: 35.2, corresponding to the removal of NH_3 and H_2O molecules). The thermal stability of **5** is higher than that of **4**, showing the hydrogen bonds between the guest molecules and the framework play an important role in stabilizing the framework of **5**.

MAS NMR spectra. NMR spectra were obtained using a Varian Infinityplus-400 spectrometer with 4 mm ZrO_2 rotors. ^{27}Al MAS NMR spectra were recorded at 104.3 MHz using a 0.40 μs (π/15) pulse with a 1s recycle delay and 256 scans. A 1% aqueous $Al(H_2O)_6^{3+}$ solution was used as a reference of chemical shifts, and samples were spun at 14 kHz. ^{11}B MAS NMR spectra were recorded at 128.3 MHz

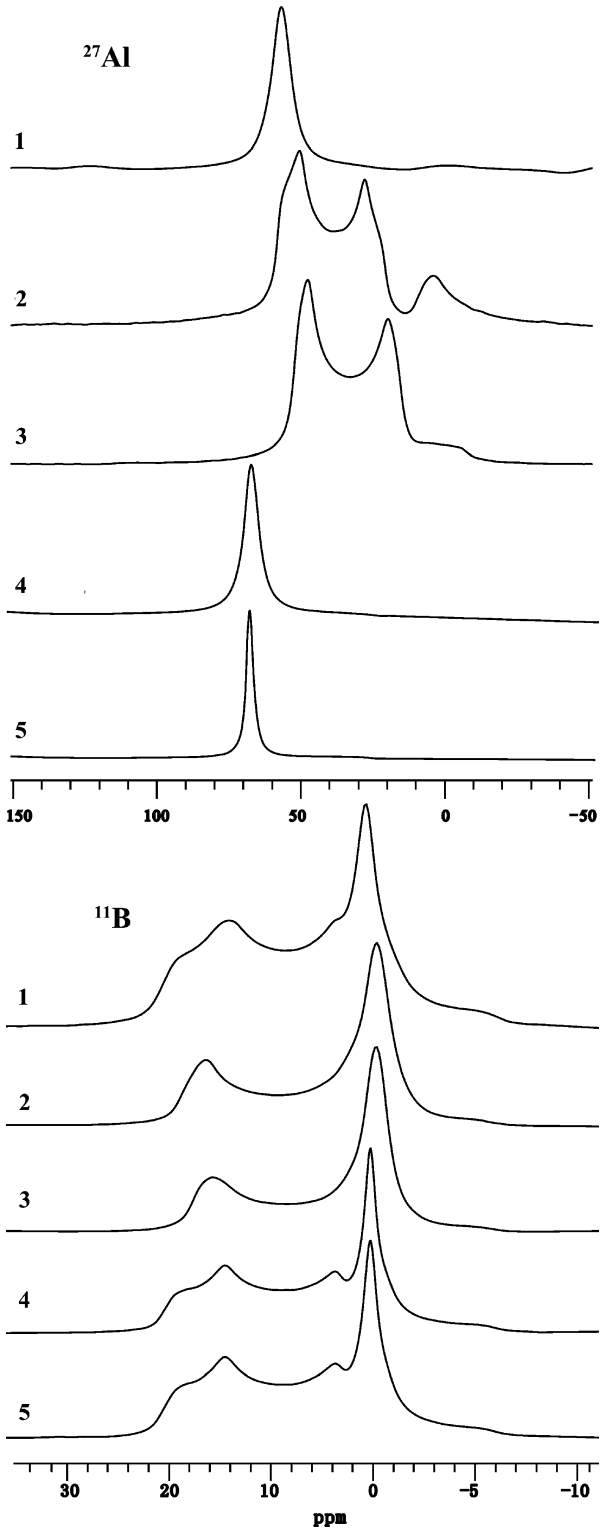

Figure 8. ^{27}Al and ^{11}B MAS NMR spectra for **1**−**5**.

using a 0.30 μs (π/15) pulse with a 1 s recycle delay and 128 scans. A 1% aqueous H_3BO_3 solution was used as a reference of chemical shifts, and samples were spun at 14 kHz. The deconvolutions of the spectra were conducted using the DMFIT software. As shown in Figure 8, the ^{27}Al and ^{11}B MAS NMR spectra for **1**−**5** and their isotropic chemical shifts are listed in Table 3. The ^{27}Al MAS NMR spectra can be divided into the following two kinds: **1**, **4**, and **5** have a

Table 3. NMR Parameters for Compounds **1**−**5**

compounds	structural units	C_Q (MHz)	η	δ_{iso} (ppm)
1	BO_3	2.70	0.35	18.2
	BO_4			1.6
	AlO_4			56.5
2	BO_3	2.62	0.11	17.8
	BO_4			1.1
	AlO_4			50.5
3	BO_3	2.60	0.09	17.3
	BO_4			1.3
	AlO_4			48.2
4	BO_3	2.72	0.15	18.3
	BO_4			1.4
	AlO_4			66.3
5	BO_3	2.62	0.34	18.2
	BO_4			1.3
	AlO_4			66.6

similarly single response peak at 56.5, 66.3, and 66.6 ppm, respectively, which are assigned to four-coordinated Al centers. The results correspond to the similar coordination environment of Al atoms in **1**, **4**, and **5** (each Al atom is coordinated by four μ_2-O atoms from four B_5O_{10} cluster units, Figure 2b). However, **2** and **3** have three response peaks at 50.5, 29.3, and 4.5 ppm for **2** and peaks at 48.2, 20.0, and 2.5 ppm for **3**, which are all attributed to four-coordinated Al centers. Different from **1**, **4**, and **5**, the Al atoms in **2** and **3** are coordinated by two μ_2-O atoms (O1, O4) from two B_4O_9 groups, one μ_3-O10 from another B_4O_9 unit, and one μ_2-O_9 from a BO_3 triangle (Figure 3a). Therefore, the Al atoms in **2** and **3** are surrounded by three types of different coordination oxygen atoms, which resulted in three different NMR signals. Because the three-coordinated B atoms are governed by a second-order nuclear electric quadrupolar interaction, the ^{11}B MAS NMR spectra in BO_3 units exhibited complex patterns in these compounds. Their quadrupolar coupling constants (C_Q) and asymmetric parameters (η) agreed well with the reported ones.[28] In addition, the sharp peaks observed around 2 ppm are attributable to the tetrahedrally coordinated boron atoms. Because of their more symmetric local environment, their ^{11}B resonances in BO_4 units are sharp and unaffected by second-order quadrupolar effects.

Conclusions

In summary, four novel acentric aluminoborate open-framework compounds with good SHG properties have been successfully made by the synergistic combination between the chiral Al centers from the hydrolysis of Al(*i*-PrO)$_3$ and the acentric borate clusters formed in situ under hydrothermal conditions. The key points of the synthetic procedures have been well established. The frameworks of **1**, **4**, and **5** are constructed from AlO_4 tetrahedra and B_5O_{10} clusters, but the topology net of **1** is different from **4** and **5**. Distinguished from **1**, **4**, and **5**, the frameworks of **2** and **3** are built up from the [Al(B_4O_9)(BO)] cluster units. The framework of **1** contains 12-, 8-, and 11-MR 3D-intersecting channel systems. It is the first example

(28) (a) Epping, J. D.; Strojek, W.; Eckert, H. *Phys. Chem. Chem. Phys.* **2005**, *7*, 2834. (b) Chan, J. C. C.; Bertmer, M.; Eckert, H. *J. Am. Chem. Soc.* **1999**, *121*, 5238.

in which three intersecting odd 11-ring channels are present among the aluminoborates. Apart from **1**, the compounds **2**−**5** crystallize in acentric structures. NLO determination shows they have good NLO activity with SHG efficiency of about 1.9, 2.1, 2.0, and 2.0 times higher than that of KDP. The UV spectra investigation and theoretical calculation indicate they are wide-band-gap semiconductors. They can emit fluorescence at 487 nm showing they are potential blue light materials. Moreover, we discussed the symmetry of the five structures, showing not only the SDAs impact on the chirality and acentricity of the inorganic frameworks, but also that the chiral/acentric inorganic groups govern the chirality/acentricity of the frameworks. Further work is in progress for making novel metal borate NLO materials by using larger acentric B−O clusters and chiral Al, Zn, Ge, and Cd centers under hydro(solvo)thermal conditions.

Acknowledgment. This work was supported by the National Natural Science Fund of China (no. 50872133), the NNSF for Distinguished Young Scholars of China (no. 20725101), the 973 Program (no. 2006CB932904), the Key Project from FJIRSM (no. SZD07001), the NSF of Fujian Province (no. E0510030), and the NNSF of China (no. 20821061).

Supporting Information Available: X-ray crystallographic files in CIF format for structures **1**−**5** and Figures S1−S11. This material is available free of charge via the Internet at http://pubs.acs.org.

IC802124V